

Electronic Correlations and Evolution of the Charge-Density Wave in the Kagome Metals AV_3Sb_5 ($A = K, Rb, Cs$)

Xiaoxiang Zhou,^{1,*} Yongkai Li,^{2,3,*} Xinwei Fan,^{1,*} Jiahao Hao,¹ Ying Xiang,¹
Zhe Liu,¹ Yaomin Dai,^{1,†} Zhiwei Wang,^{2,3,‡} Yugui Yao,^{2,3} and Hai-Hu Wen^{1,§}

¹*National Laboratory of Solid State Microstructures and Department of Physics,
Collaborative Innovation Center of Advanced Microstructures, Nanjing University, Nanjing 210093, China*

²*Key Laboratory of Advanced Optoelectronic Quantum Architecture and Measurement,
Ministry of Education, School of Physics, Beijing Institute of Technology, Beijing 100081, China*

³*Micronano Center, Beijing Key Lab of Nanophotonics and Ultrafine Optoelectronic Systems,
Beijing Institute of Technology, Beijing 100081, China*

(Dated: August 23, 2022)

The kagome metals AV_3Sb_5 ($A = K, Rb, Cs$) have attracted enormous interest as they exhibit intertwined charge-density wave (CDW) and superconductivity. The alkali-metal dependence of these characteristics contains pivotal information about the CDW and its interplay with superconductivity. Here, we report optical studies of AV_3Sb_5 across the whole family. With increasing alkali-metal atom radius from K to Cs, the CDW gap increases monotonically, whereas T_{CDW} first rises and then drops, at variance with conventional CDW. While the Fermi surface gapped by the CDW grows, T_c is elevated in CsV_3Sb_5 , indicating that the interplay between the CDW and superconductivity is not simply a competition for the density of states near E_F . More importantly, we observe an enhancement of electronic correlations in CsV_3Sb_5 , which suppresses the CDW but enhances superconductivity, thus accounting for the above peculiar observations. Our results suggest electronic correlations as an important factor in manipulating the CDW and its entanglement with superconductivity in AV_3Sb_5 .

The kagome lattice, composed of hexagons and corner-sharing triangles, provides a fascinating playground for exploring exotic quantum phenomena. For instance, spins or magnetic moments on a kagome lattice are subject to high degree of geometric frustration that may lead to quantum spin liquids [1, 2]; electrons in a kagome lattice form flat bands, Dirac points, and saddle points, which support intriguing quantum phenomena associated with nontrivial band topology [3–7] and a wide variety of electronic instabilities [8–11]. Particularly at van Hove filling, as a function of the on-site repulsion U and nearest-neighbor Coulomb interaction V , the kagome lattice exhibits a rich phase diagram consisting of various phases such as charge or spin bond order [10, 11], unconventional superconductivity [8, 10, 11], charge-density wave (CDW) [11], and spin-density wave (SDW) [8].

The recently discovered kagome metals AV_3Sb_5 ($A = K, Rb, Cs$) [12] with the Fermi level E_F lying near the saddle points (van Hove filling) provide an excellent platform to realize the above exotic quantum states in real materials. Multiple topologically protected Dirac bands [13, 14] and superconductivity with a transition temperature T_c of 0.92–2.5 K [13–15] have been reported in these compounds. In addition, a CDW transition occurs at $T_{CDW} = 78, 103,$ and 94 K for $KV_3Sb_5,$ $RbV_3Sb_5,$ and $CsV_3Sb_5,$ respectively [12–15], resulting in a three-dimensional (3D) $2 \times 2 \times 2$ superlattice [16, 17]. Upon entering the CDW state, a giant anomalous Hall effect [18, 19] and electronic nematicity [20–23] also emerge. The application of pressure [24–27], uniaxial strain [28], or chemical doping [29–32] suppresses the

CDW order, but enhances the superconductivity, signifying the competition between the CDW and superconductivity in AV_3Sb_5 . While a variety of studies suggest that the saddle point or Fermi surface (FS) nesting plays an important role in driving the CDW instability [33–40], there is also evidence that the CDW phase is mainly driven by electron-phonon (e-ph) coupling [41–44]. At the present time, the driving mechanism of the CDW and how it interacts with superconductivity in AV_3Sb_5 are subjects for intensive debate.

The evolution of the CDW and superconducting properties with alkali metal in AV_3Sb_5 may reveal key information about the factors controlling the CDW order and its interplay with superconductivity. In this Letter, we systematically study the optical properties of AV_3Sb_5 across the whole family. As the alkali-metal atom radius grows from K to Cs, the CDW gap Δ_{CDW} increases monotonically, whereas T_{CDW} first rises but then drops, failing to exhibit a scaling relation with Δ_{CDW} . This anomalous behavior is clearly at odds with the description of conventional CDW order. While the FS removed by Δ_{CDW} increases, T_c is raised in CsV_3Sb_5 , indicating that the interplay between the CDW and superconductivity is not simply a competition for the density of states (DOS) near E_F . Moreover, we observe an enhancement of electronic correlations in CsV_3Sb_5 , which suppresses the CDW but promotes unconventional superconductivity, giving rise to the above peculiar behavior. Our results underline the importance of electronic correlations in manipulating the CDW and its entanglement with superconductivity in AV_3Sb_5 .

arXiv:2208.09804v1 [cond-mat.supr-con] 21 Aug 2022

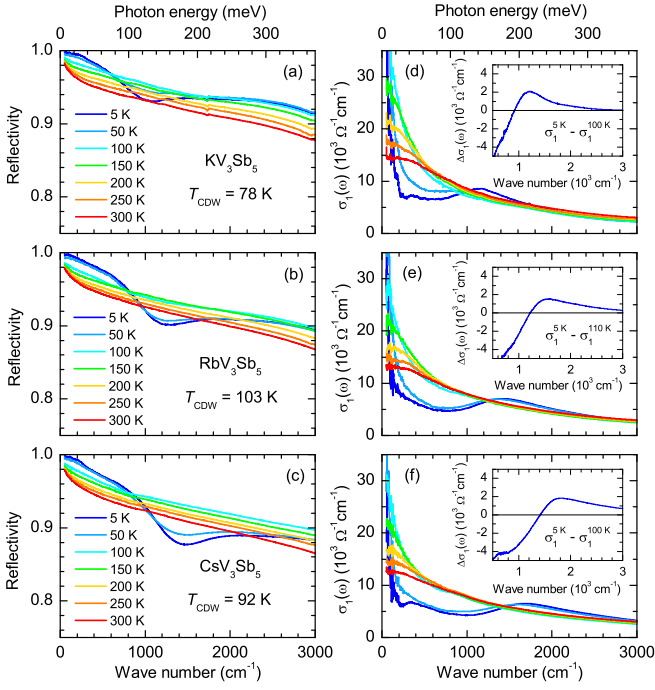


Figure 1. (a)–(c) $R(\omega)$ at several representative temperatures for KV_3Sb_5 , RbV_3Sb_5 , and CsV_3Sb_5 , respectively. (d)–(f) $\sigma_1(\omega)$ for KV_3Sb_5 , RbV_3Sb_5 , and CsV_3Sb_5 , respectively. The inset displays $\Delta\sigma_1(\omega)$ at 5 K for each compound, where $\sigma_1(\omega)$ at T just above T_{CDW} is used as the base curve.

High-quality single crystals of AV_3Sb_5 ($A = K, Rb, Cs$) were synthesized using the self-flux method and characterized by x-ray diffraction [45]. Transport measurements were carried out to confirm the CDW transition at $T_{CDW} = 78, 103,$ and 92 K in $KV_3Sb_5, RbV_3Sb_5,$ and CsV_3Sb_5 , respectively [45]. The details of optical measurements can be found in the Supplemental Material [45].

Figures 1(a)–1(c) show the measured reflectivity $R(\omega)$ up to 3000 cm^{-1} at several representative temperatures for $KV_3Sb_5, RbV_3Sb_5,$ and CsV_3Sb_5 , respectively. Above T_{CDW} , $R(\omega)$ for all three compounds exhibits metallic behavior: a very high $R(\omega)$ in the far-infrared range that approaches unity in the zero-frequency limit and increases with decreasing T . Below T_{CDW} , a suppression of $R(\omega)$ in the frequency range of $1000\text{--}1500\text{ cm}^{-1}$ occurs for all three materials, signaling the opening of a CDW gap. As the radius of the alkali-metal atom grows from K to Cs, the suppression in $R(\omega)$ shifts to higher frequency and deepens, suggesting that the CDW gap increases in energy and the gap-induced FS modification intensifies with growing alkali-metal atom radius.

Figures 1(d)–1(f) show the optical conductivity $\sigma_1(\omega)$ at several representative temperatures above and below T_{CDW} for $KV_3Sb_5, RbV_3Sb_5,$ and CsV_3Sb_5 , respectively. For all three compounds, above T_{CDW} , a Drude response, i.e. a peak centered at zero frequency, can be clearly observed in the low-frequency $\sigma_1(\omega)$, in good agreement

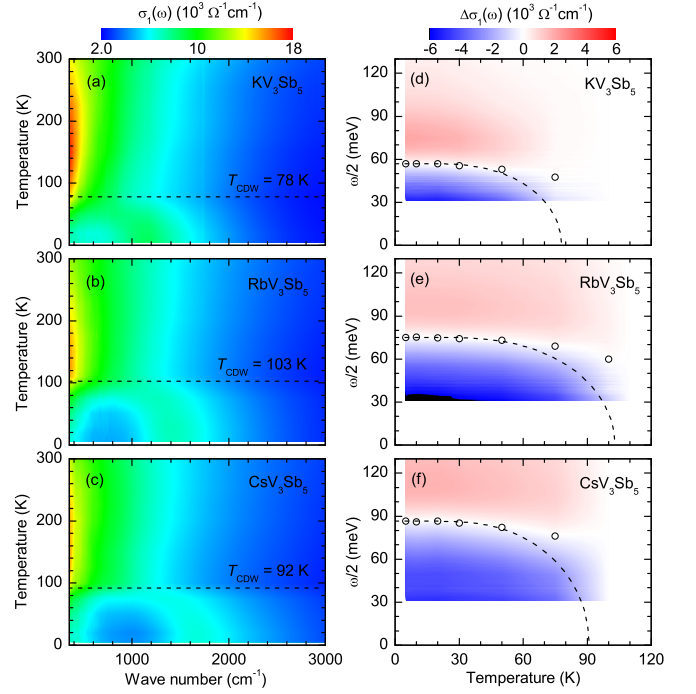


Figure 2. (a)–(c) The 2D T - ω map of $\sigma_1(\omega)$ for $KV_3Sb_5, RbV_3Sb_5,$ and CsV_3Sb_5 , respectively. The horizontal dashed line in each panel denotes T_{CDW} . (d)–(f) $\Delta\sigma_1(\omega)$ in the 2D $\omega/2$ - T plot, where the white color (zero crossing points) yields the T dependence of Δ_{CDW} . The dashed line in each panel represents the mean-field behavior.

with the metallic nature of these materials; below T_{CDW} , a dramatic suppression of the low-frequency $\sigma_1(\omega)$ sets in, and the removed spectral weight [the area under $\sigma_1(\omega)$] is transferred to higher frequencies, which is the prototypical response of the CDW gap in $\sigma_1(\omega)$. The detailed evolution of $\sigma_1(\omega)$ with T is traced out in the 2D temperature-frequency (T - ω) maps in Figs. 2(a)–2(c) for all three materials. The horizontal dashed line in each panel denotes T_{CDW} for $KV_3Sb_5, RbV_3Sb_5,$ and CsV_3Sb_5 , respectively. Below T_{CDW} , the opening of the CDW gap leads to the presence of a blue region in the low-frequency range [a suppression of the low-frequency $\sigma_1(\omega)$] and a shift of the green/cyan region to higher frequencies. A comparison of Figs. 2(a)–2(c) reveals that as the radius of the alkali-metal atom in AV_3Sb_5 increases, the low-frequency blue region moves to higher frequencies and grows in area. These observations indicate that not only does the CDW gap value increase, the removed spectral weight due to the opening of the CDW gap also grows with increasing alkali-metal atom radius.

The CDW gap Δ_{CDW} can be determined from the zero-crossing point in the difference optical conductivity,

$$\Delta\sigma_1(\omega) = \sigma_1^{T < T_{CDW}}(\omega) - \sigma_1^N(\omega), \quad (1)$$

where $\sigma_1^{T < T_{CDW}}(\omega)$ represents $\sigma_1(\omega)$ at $T < T_{CDW}$; $\sigma_1^N(\omega)$ refers to $\sigma_1(\omega)$ in the normal state, namely at

T slightly above T_{CDW} . The insets of Figs. 1(d)–1(f) display $\Delta\sigma_1(\omega)$ at 5 K for KV_3Sb_5 , RbV_3Sb_5 , and CsV_3Sb_5 , respectively, in which the zero-crossing point corresponds to $2\Delta_{\text{CDW}}$. Therefore, the T dependence of Δ_{CDW} can be obtained by plotting $\Delta\sigma_1(\omega)$ in the 2D $\omega/2$ - T maps as shown in Figs. 2(d)–2(f) for KV_3Sb_5 , RbV_3Sb_5 , and CsV_3Sb_5 , respectively. In each panel, while the red and blue colors denote positive and negative values for $\Delta\sigma_1(\omega)$, the white color corresponds to the zero-crossing points which yields the evolution of Δ_{CDW} with T . For all three materials, the T dependence of Δ_{CDW} deviates from the BCS mean-field behavior (black dashed line) in the proximity of T_{CDW} , consistent with previous studies [35, 46, 47]. This implies that the CDW transition in AV_3Sb_5 is unconventional and most likely to be of the first order, in accord with recent NMR studies [48–50]. Moreover, Δ_{CDW} increases monotonically with increasing alkali-metal atom radius, failing to show a scaling relation with T_{CDW} which increases in RbV_3Sb_5 but then drops in CsV_3Sb_5 . The values of Δ_{CDW} and T_{CDW} for AV_3Sb_5 are summarized in Figs. 4(a) and 4(b), respectively, for further discussions.

The removed spectral weight ΔS in the low-frequency range due to the opening of Δ_{CDW} reflects the gapped portion of the FS or the reduction of the density of states (DOS) near E_{F} . ΔS can be directly obtained from the integral of $\sigma_1(\omega)$,

$$\Delta S = \int_0^{2\Delta_{\text{CDW}}} [\sigma_1^N(\omega) - \sigma_1^{T < T_{\text{CDW}}}(\omega)] d\omega, \quad (2)$$

The values of ΔS at $T = 5$ K determined from Eq. (2) are 6.00, 6.49, and $6.74 \times 10^6 \Omega^{-1}\text{cm}^{-2}$ for KV_3Sb_5 , RbV_3Sb_5 , and CsV_3Sb_5 , respectively. The increase of ΔS with increasing alkali-metal atom radius indicates that a larger portion of the FS is removed by Δ_{CDW} in AV_3Sb_5 with a larger alkali-metal atom. We plot ΔS at $T = 5$ K as a function of alkali metal in Fig. 4(d) for further discussions.

The ratio of the experimental kinetic energy K_{exp} to the kinetic energy from band theory K_{band} provides crucial information about the electronic correlations in AV_3Sb_5 [51–53]. The electron's kinetic energy can be conveniently derived from the area under the Drude feature in $\sigma_1(\omega)$ [51, 52],

$$K = \frac{2\hbar^2 c_0}{\pi e^2} \int_0^{\omega_c} \sigma_1(\omega) d\omega, \quad (3)$$

where c_0 is the distance between the V kagome layers, and ω_c is a cutoff frequency covering the entire Drude component in $\sigma_1(\omega)$. In order to determine K_{band} , we calculated the ab -plane $\sigma_1(\omega)$ for all three materials [45]. As depicted in Figs. 3(a)–3(c), the calculated $\sigma_1(\omega)$ spectra (blue curves) qualitatively agree with the measured ones (red curves). Using $\omega_c = 5000 \text{ cm}^{-1}$ for both the measured and the calculated $\sigma_1(\omega)$, the values of $K_{\text{exp}}/K_{\text{band}}$ are obtained for all three compounds.

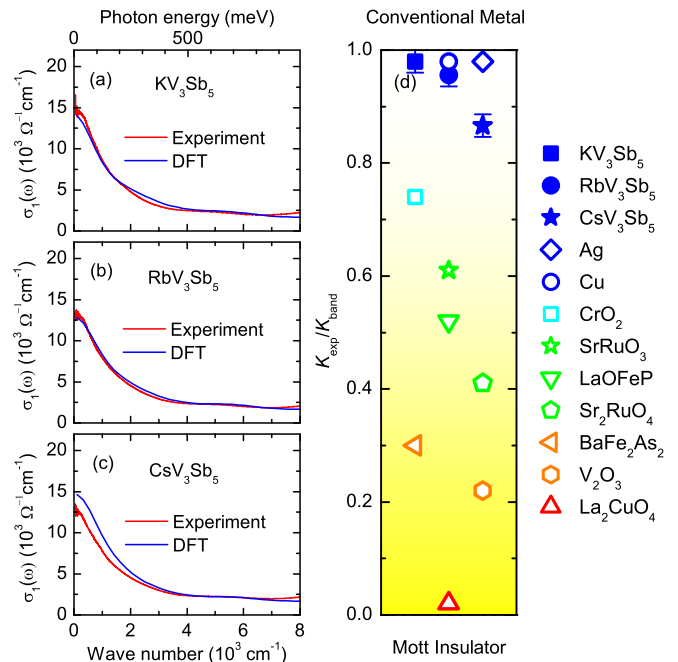


Figure 3. (a)–(c) Comparison between the calculated $\sigma_1(\omega)$ (blue solid curve) and the measured $\sigma_1(\omega)$ at 300 K (red solid curve) for KV_3Sb_5 , RbV_3Sb_5 , and CsV_3Sb_5 , respectively. (d) $K_{\text{exp}}/K_{\text{band}}$ for AV_3Sb_5 (solid symbols) and several other representative materials (open symbols). The values of $K_{\text{exp}}/K_{\text{band}}$ for other materials are obtained from Ref. [51] and the references cited therein.

Figure 3(d) summarizes $K_{\text{exp}}/K_{\text{band}}$ for AV_3Sb_5 (solid symbols) and some other representative materials (open symbols). While conventional metals, such as Ag and Cu, have $K_{\text{exp}}/K_{\text{band}}$ close to unity, $K_{\text{exp}}/K_{\text{band}}$ for the well-known Mott insulator, such as La_2CuO_4 , is almost zero due to on-site Coulomb repulsion which impedes the motion of electrons. Iron pnictides, e.g. LaOFeP and BaFe_2As_2 , are categorized as moderately correlated materials, as their $K_{\text{exp}}/K_{\text{band}}$ lies between conventional metals and Mott insulators. The values of $K_{\text{exp}}/K_{\text{band}}$ for KV_3Sb_5 (solid square), RbV_3Sb_5 (solid circle), and CsV_3Sb_5 (solid star) fall into the range of 0.86–0.98, indicating that the electronic correlations in AV_3Sb_5 is weak in general. However, it's worth noting that while the values of $K_{\text{exp}}/K_{\text{band}}$ in KV_3Sb_5 and RbV_3Sb_5 are close to that in conventional metals, CsV_3Sb_5 features a reduced $K_{\text{exp}}/K_{\text{band}}$, signifying an enhancement of electronic correlations. Theoretical calculations have revealed that the FS of AV_3Sb_5 is formed by Sb-5p and V-3d orbitals [33, 54, 55]. Since 3d electrons are subject to strong electronic correlations [56, 57], the electronic correlations in AV_3Sb_5 are likely to arise from the V-3d orbitals. Here, both K_{exp} and K_{band} consist of contributions from all orbitals at E_{F} , including the weakly correlated Sb-5p orbital, so the actual electronic correlations in the V-3d orbitals are stronger than that determined

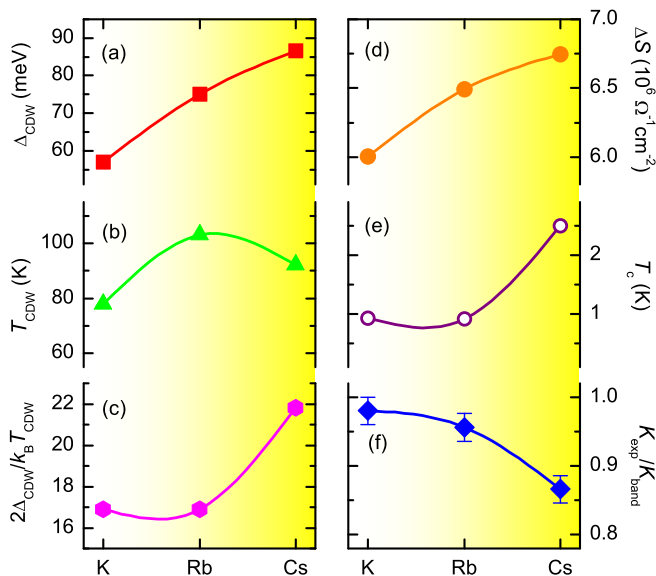


Figure 4. The evolution of (a) Δ_{CDW} , (b) T_{CDW} , (c) $2\Delta_{\text{CDW}}/k_{\text{B}}T_{\text{CDW}}$, (d) ΔS , (e) T_{c} , and (f) $K_{\text{exp}}/K_{\text{band}}$ with the alkali-metal atom in the $AV_3\text{Sb}_5$ family.

from $K_{\text{exp}}/K_{\text{band}}$. Given that the ground state of the kagome lattice sensitively depends on electronic correlations [10, 11, 34], the enhancement of electronic correlations in CsV_3Sb_5 , although not as strong as that in cuprates and iron pnictides, may have an important influence on the CDW and its interplay with superconductivity. For further discussions, the evolution of $K_{\text{exp}}/K_{\text{band}}$ with alkali metal is traced out in Fig. 4(f).

Essential information about the CDW and how it intertwines with superconductivity in $AV_3\text{Sb}_5$ can be obtained from the alkali-metal dependence of the experimentally determined parameters, which has been summarized in Figs. 4(a)–4(f). A noticeable yet puzzling observation is that while Δ_{CDW} [Fig. 4(a)] increases monotonically with increasing alkali-metal atom radius, T_{CDW} [Fig. 4(b)] first increases but then decreases, failing to establish a scaling relation with Δ_{CDW} . This anomalous behavior is clearly at odds with the conventional description of CDW order [58]. Figure 4(c) shows that KV_3Sb_5 and RbV_3Sb_5 have the same $2\Delta_{\text{CDW}}/k_{\text{B}}T_{\text{CDW}}$, indicating that the CDW is governed by the same mechanism in these two compounds, whereas $2\Delta_{\text{CDW}}/k_{\text{B}}T_{\text{CDW}}$ is significantly larger in CsV_3Sb_5 , suggesting that an extra factor is acting on the CDW order. Thus far, the driving force of the CDW order in $AV_3\text{Sb}_5$ is still highly controversial. Extensive studies hint that the CDW instability in $AV_3\text{Sb}_5$ is driven by the nesting of the FS or saddle points [33–40], but on the other hand, a recent ARPES study on KV_3Sb_5 [41], neutron scattering [42] and Raman [44] measurements on CsV_3Sb_5 suggest that e-ph coupling plays a dominant role in driving the CDW instability in $AV_3\text{Sb}_5$. Nevertheless, for both the nest-

ing driven and e-ph coupling driven scenarios, a larger Δ_{CDW} would naturally support a higher T_{CDW} . Here in CsV_3Sb_5 , an increase of Δ_{CDW} coincides with a decrease of T_{CDW} , implying that besides e-ph coupling and FS nesting which should enhance both Δ_{CDW} and T_{CDW} , a competing factor that suppresses T_{CDW} also exerts considerable influence on the CDW order. Previous studies on transition metal dichalcogenides have documented that while e-ph coupling, FS nesting, and a high DOS are beneficial to the formation of CDW order, electronic correlations act as a competing factor which tends to localize the carriers and prevents the formation of CDW order [59, 60]. Our optical results have attested to the decrease of $K_{\text{exp}}/K_{\text{band}}$ [Fig. 4(f)], i.e. the enhancement of electronic correlations in CsV_3Sb_5 . These facts bring us to the possibility that the suppression of T_{CDW} and the larger $2\Delta_{\text{CDW}}/k_{\text{B}}T_{\text{CDW}}$ in CsV_3Sb_5 may be related to the enhancement of electronic correlations.

Other interesting observations emerge from the comparison of T_{c} , T_{CDW} , ΔS , and $2\Delta_{\text{CDW}}/k_{\text{B}}T_{\text{CDW}}$. As shown in Figs. 4(b) and 4(e), the suppression of T_{CDW} in CsV_3Sb_5 is accompanied by an enhancement of T_{c} , in accord with the competition relation between the CDW and superconductivity reported by previous work [24–30]. The competition between the CDW and superconductivity is not surprising, because the opening of the CDW gap depletes the DOS near E_{F} , resulting in a suppression of superconductivity. However, the comparison of Figs. 4(d) and 4(e) reveals that the rise of T_{c} in CsV_3Sb_5 coincides with an increase of ΔS . This observation implies that the CDW instability and superconductivity in $AV_3\text{Sb}_5$ do not share the same DOS, so that the competition between the CDW and superconductivity is not simply through competing for effective DOS near E_{F} , but controlled by another factor. Furthermore, $2\Delta_{\text{CDW}}/k_{\text{B}}T_{\text{CDW}}$ [Fig. 4(c)] and T_{c} [Fig. 4(e)] exhibit identical alkali-metal dependence, hinting that the suppression of T_{CDW} and the enhancement of T_{c} in CsV_3Sb_5 are most likely induced by the same factor, namely electronic correlations. A recent theoretical study has shown that electronic correlations suppress the charge susceptibility but significantly enhance the spin susceptibility or spin fluctuations [59], which are believed to mediate unconventional superconductivity [61]. Moreover, extensive studies on cuprates and iron pnictides have underlined the importance of electronic correlations in generating unconventional superconductivity [57, 62]. Combining these studies with our observations, we suggest that electronic correlations should be taken into account when constructing a theory to describe the CDW phase and its entanglement with superconductivity in $AV_3\text{Sb}_5$.

To summarize, we performed a systematic investigation into the optical properties of $AV_3\text{Sb}_5$ ($A = \text{K}, \text{Rb}, \text{Cs}$) across the whole family. We found that as the alkali-metal atom radius grows from K to Cs, (i) while Δ_{CDW} increases monotonically, T_{CDW} rises in RbV_3Sb_5 but then

drops in CsV_3Sb_5 , at odds with conventional CDW; (ii) the FS removed by Δ_{CDW} increases, whereas T_c is enhanced in CsV_3Sb_5 , suggesting that the interplay between the CDW and superconductivity is not simply a competition for effective DOS near E_F ; (iii) $K_{\text{exp}}/K_{\text{band}}$ is reduced, indicating an enhancement of electronic correlations. An analysis considering all the above observations and previous work suggests that the enhancement of electronic correlations may be a decisive factor that controls the formation of the CDW order and its entanglement with superconductivity in AV_3Sb_5 .

We thank Hu Miao, R. Thomale, Qianghua Wang, Nanlin Wang, Xiaoxiang Xi, Bing Xu, Binghai Yan, Huan Yang, Run Yang, Shunli Yu, Peng Zhang, and Jianzhou Zhao for helpful discussions. We gratefully acknowledge financial support from the National Key R&D Program of China (Grants No. 2016YFA0300401 and 2020YFA0308800), the National Natural Science Foundation of China (Grants No. 11874206, 12061131001, 92065109, 11734003 and 11904294), the Fundamental Research Funds for the Central Universities (Grant No. 020414380095), Jiangsu shuangchuang program, the Beijing Natural Science Foundation (Grant No. Z190006 and Z210006), and the Beijing Institute of Technology Research Fund Program for Young Scholars (Grant No. 3180012222011).

* These authors contributed equally to this work.

† ymdai@nju.edu.cn

‡ zhiweiwang@bit.edu.cn

§ hhwen@nju.edu.cn

- [1] L. Balents, *Nature* **464**, 199 (2010).
- [2] S. Yan, D. A. Huse, and S. R. White, *Science* **332**, 1173 (2011).
- [3] I. I. Mazin, H. O. Jeschke, F. Lechermann, H. Lee, M. Fink, R. Thomale, and R. Valentí, *Nat. Commun.* **5**, 4261 (2014).
- [4] L. Ye, M. Kang, J. Liu, F. von Cube, C. R. Wicker, T. Suzuki, C. Jozwiak, A. Bostwick, E. Rotenberg, D. C. Bell, et al., *Nature* **555**, 638 (2018).
- [5] M. Kang, L. Ye, S. Fang, J.-S. You, A. Levitan, M. Han, J. I. Facio, C. Jozwiak, A. Bostwick, E. Rotenberg, et al., *Nat. Mat.* **19**, 163 (2020).
- [6] M. Kang, S. Fang, L. Ye, H. C. Po, J. Denlinger, C. Jozwiak, A. Bostwick, E. Rotenberg, E. Kaxiras, J. G. Checkelsky, et al., *Nat. Commun.* **11**, 4004 (2020).
- [7] Z. Liu, M. Li, Q. Wang, G. Wang, C. Wen, K. Jiang, X. Lu, S. Yan, Y. Huang, D. Shen, et al., *Nat. Commun.* **11**, 4002 (2020).
- [8] S.-L. Yu and J.-X. Li, *Phys. Rev. B* **85**, 144402 (2012).
- [9] M. L. Kiesel and R. Thomale, *Phys. Rev. B* **86**, 121105 (2012).
- [10] M. L. Kiesel, C. Platt, and R. Thomale, *Phys. Rev. Lett.* **110**, 126405 (2013).
- [11] W.-S. Wang, Z.-Z. Li, Y.-Y. Xiang, and Q.-H. Wang, *Phys. Rev. B* **87**, 115135 (2013).
- [12] B. R. Ortiz, L. C. Gomes, J. R. Morey, M. Winiarski, M. Bordelon, J. S. Mangum, I. W. H. Oswald, J. A. Rodriguez-Rivera, J. R. Neilson, S. D. Wilson, et al., *Phys. Rev. Materials* **3**, 094407 (2019).
- [13] B. R. Ortiz, S. M. L. Teicher, Y. Hu, J. L. Zuo, P. M. Sarte, E. C. Schueller, A. M. M. Abeykoon, M. J. Krogstad, S. Rosenkranz, R. Osborn, et al., *Phys. Rev. Lett.* **125**, 247002 (2020).
- [14] Q. Yin, Z. Tu, C. Gong, Y. Fu, S. Yan, and H. Lei, *Chin. Phys. Lett.* **38**, 037403 (2021).
- [15] B. R. Ortiz, P. M. Sarte, E. M. Kenney, M. J. Graf, S. M. L. Teicher, R. Seshadri, and S. D. Wilson, *Phys. Rev. Mater.* **5**, 034801 (2021).
- [16] Z. Liang, X. Hou, F. Zhang, W. Ma, P. Wu, Z. Zhang, F. Yu, J.-J. Ying, K. Jiang, L. Shan, et al., *Phys. Rev. X* **11**, 031026 (2021).
- [17] H. Li, T. T. Zhang, T. Yilmaz, Y. Y. Pai, C. E. Marvinney, A. Said, Q. W. Yin, C. S. Gong, Z. J. Tu, E. Vescovo, et al., *Phys. Rev. X* **11**, 031050 (2021).
- [18] S.-Y. Yang, Y. Wang, B. R. Ortiz, D. Liu, J. Gayles, E. Derunova, R. Gonzalez-Hernandez, L. Šmejkal, Y. Chen, S. S. P. Parkin, et al., *Sci. Adv.* **6**, eabb6003 (2020).
- [19] F. H. Yu, T. Wu, Z. Y. Wang, B. Lei, W. Z. Zhuo, J. J. Ying, and X. H. Chen, *Phys. Rev. B* **104**, L041103 (2021).
- [20] Y. Xiang, Q. Li, Y. Li, W. Xie, H. Yang, Z. Wang, Y. Yao, and H.-H. Wen, *Nat. Commun.* **12**, 6727 (2021).
- [21] H. Chen, H. Yang, B. Hu, Z. Zhao, J. Yuan, Y. Xing, G. Qian, Z. Huang, G. Li, Y. Ye, et al., *Nature* **599**, 222 (2021).
- [22] H. Li, H. Zhao, B. R. Ortiz, T. Park, M. Ye, L. Balents, Z. Wang, S. D. Wilson, and I. Zeljkovic, *Nat. Phys.* **18**, 265 (2022).
- [23] Q. Wu, Z. X. Wang, Q. M. Liu, R. S. Li, S. X. Xu, Q. W. Yin, C. S. Gong, Z. J. Tu, H. C. Lei, T. Dong, et al. (2021), arXiv:2110.11306.
- [24] F. H. Yu, D. H. Ma, W. Z. Zhuo, S. Q. Liu, X. K. Wen, B. Lei, J. J. Ying, and X. H. Chen, *Nat. Commun.* **12**, 3645 (2021).
- [25] K. Y. Chen, N. N. Wang, Q. W. Yin, Y. H. Gu, K. Jiang, Z. J. Tu, C. S. Gong, Y. Uwatoko, J. P. Sun, H. C. Lei, et al., *Phys. Rev. Lett.* **126**, 247001 (2021).
- [26] F. Du, S. Luo, B. R. Ortiz, Y. Chen, W. Duan, D. Zhang, X. Lu, S. D. Wilson, Y. Song, and H. Yuan, *Phys. Rev. B* **103**, L220504 (2021).
- [27] Z. Zhang, Z. Chen, Y. Zhou, Y. Yuan, S. Wang, J. Wang, H. Yang, C. An, L. Zhang, X. Zhu, et al., *Phys. Rev. B* **103**, 224513 (2021).
- [28] T. Qian, M. H. Christensen, C. Hu, A. Saha, B. M. Andersen, R. M. Fernandes, T. Birol, and N. Ni, *Phys. Rev. B* **104**, 144506 (2021).
- [29] Y. Song, T. Ying, X. Chen, X. Han, X. Wu, A. P. Schnyder, Y. Huang, J.-g. Guo, and X. Chen, *Phys. Rev. Lett.* **127**, 237001 (2021).
- [30] Y. M. Oey, B. R. Ortiz, F. Kaboudvand, J. Frassinetti, E. Garcia, R. Cong, S. Sanna, V. F. Mitrović, R. Seshadri, and S. D. Wilson, *Phys. Rev. Materials* **6**, L041801 (2022).
- [31] Y. Li, Q. Li, X. Fan, J. Liu, Q. Feng, M. Liu, C. Wang, J.-X. Yin, J. Duan, X. Li, et al., *Phys. Rev. B* **105**, L180507 (2022).
- [32] Y. Liu, Y. Wang, Y. Cai, Z. Hao, X.-M. Ma, L. Wang, C. Liu, J. Chen, L. Zhou, J. Wang, et al. (2021), arXiv:2110.12651.

- [33] H. Tan, Y. Liu, Z. Wang, and B. Yan, Phys. Rev. Lett. **127**, 046401 (2021).
- [34] M. M. Denner, R. Thomale, and T. Neupert, Phys. Rev. Lett. **127**, 217601 (2021).
- [35] X. Zhou, Y. Li, X. Fan, J. Hao, Y. Dai, Z. Wang, Y. Yao, and H.-H. Wen, Phys. Rev. B **104**, L041101 (2021).
- [36] M. H. Christensen, T. Birol, B. M. Andersen, and R. M. Fernandes, Phys. Rev. B **104**, 214513 (2021).
- [37] Z. Wang, S. Ma, Y. Zhang, H. Yang, Z. Zhao, Y. Ou, Y. Zhu, S. Ni, Z. Lu, H. Chen, et al. (2021), arXiv:2104.05556.
- [38] S. Cho, H. Ma, W. Xia, Y. Yang, Z. Liu, Z. Huang, Z. Jiang, X. Lu, J. Liu, Z. Liu, et al., Phys. Rev. Lett. **127**, 236401 (2021).
- [39] R. Lou, A. Fedorov, Q. Yin, A. Kuibarov, Z. Tu, C. Gong, E. F. Schwier, B. Büchner, H. Lei, and S. Borisenko, Phys. Rev. Lett. **128**, 036402 (2022).
- [40] T. M. Rice and G. K. Scott, Phys. Rev. Lett. **35**, 120 (1975).
- [41] H. Luo, Q. Gao, H. Liu, Y. Gu, D. Wu, C. Yi, J. Jia, S. Wu, X. Luo, Y. Xu, et al., Nat. Commun. **13**, 273 (2022).
- [42] Y. Xie, Y. Li, P. Bourges, A. Ivanov, Z. Ye, J.-X. Yin, M. Z. Hasan, A. Luo, Y. Yao, Z. Wang, et al., Phys. Rev. B **105**, L140501 (2022).
- [43] J.-G. Si, W.-J. Lu, Y.-P. Sun, P.-F. Liu, and B.-T. Wang, Phys. Rev. B **105**, 024517 (2022).
- [44] G. Liu, X. Ma, K. He, Q. Li, H. Tan, Y. Liu, J. Xu, W. Tang, K. Watanabe, T. Taniguchi, et al., Nat. Commun. **13**, 3461 (2022).
- [45] *See Supplemental Material for details about sample synthesis, sample characterizations, optical measurements, and first-principles calculations.*
- [46] E. Uykur, B. R. Ortiz, O. Iakutkina, M. Wenzel, S. D. Wilson, M. Dressel, and A. A. Tsirlin, Phys. Rev. B **104**, 045130 (2021).
- [47] E. Uykur, B. R. Ortiz, S. D. Wilson, M. Dressel, and A. A. Tsirlin, npj Quantum Mater. **7**, 16 (2022).
- [48] C. Mu, Q. Yin, Z. Tu, C. Gong, H. Lei, Z. Li, and J. Luo, Chin. Phys. Lett. **38**, 077402 (2021).
- [49] D. Song, L. Zheng, F. Yu, J. Li, L. Nie, M. Shan, D. Zhao, S. Li, B. Kang, Z. Wu, et al., Sci. China Phys. Mech. Astron. **65**, 247462 (2022).
- [50] J. Luo, Z. Zhao, Y. Z. Zhou, J. Yang, A. F. Fang, H. T. Yang, H. J. Gao, R. Zhou, and G.-q. Zheng, npj Quantum Mater. **7**, 30 (2022).
- [51] M. M. Qazilbash, J. J. Hamlin, R. E. Baumbach, L. Zhang, D. J. Singh, M. B. Maple, and D. N. Basov, Nat. Phys. **5**, 647 (2009).
- [52] A. J. Millis, A. Zimmers, R. P. S. M. Lobo, N. Bontemps, and C. C. Homes, Phys. Rev. B **72**, 224517 (2005).
- [53] Y. Xu, J. Zhao, C. Yi, Q. Wang, Q. Yin, Y. Wang, X. Hu, L. Wang, E. Liu, G. Xu, et al., Nat. Commun. **11**, 3985 (2020).
- [54] J. Zhao, W. Wu, Y. Wang, and S. A. Yang, Phys. Rev. B **103**, L241117 (2021).
- [55] H. LaBollita and A. S. Botana, Phys. Rev. B **104**, 205129 (2021).
- [56] M. Imada, A. Fujimori, and Y. Tokura, Rev. Mod. Phys. **70**, 1039 (1998).
- [57] R. Yu, H. Hu, E. M. Nica, J.-X. Zhu, and Q. Si, Front. Phys. **9**, 578347 (2021).
- [58] G. Grüner, Rev. Mod. Phys. **60**, 1129 (1988).
- [59] E. G. C. P. van Loon, M. Rösner, G. Schönhoff, M. I. Katsnelson, and T. O. Wehling, npj Quantum Mater. **3**, 32 (2018).
- [60] D. Lin, S. Li, J. Wen, H. Berger, L. Forró, H. Zhou, S. Jia, T. Taniguchi, K. Watanabe, X. Xi, et al., Nat. Commun. **11**, 2406 (2020).
- [61] T. Moriya and K. Ueda, Adv. Phys. **49**, 555 (2000).
- [62] P. A. Lee, N. Nagaosa, and X.-G. Wen, Rev. Mod. Phys. **78**, 17 (2006).